

Article

Biomass Gasification and Applied Intelligent Retrieval in Modeling

Manish Meena ^{1,2}, Hrishikesh Kumar ^{2,3}, Nitin Dutt Chaturvedi ¹, Andrey A. Kovalev ⁴, Vadim Bolshev ⁴, Dmitriy A. Kovalev ⁴, Prakash Kumar Sarangi ⁵, Aakash Chawade ⁶, Manish Singh Rajput ⁷, Vivekanand Vivekanand ^{2,*} and Vladimir Panchenko ^{8,*}

¹ Department of Chemical and Biochemical Engineering, Indian Institute of Technology Patna, Patna 801106, Bihar, India; manish_2221cb03@iitp.ac.in (M.M.); nitind@iitp.ac.in (N.D.C.)

² Centre for Energy and Environment, Malaviya National Institute of Technology Jaipur, Jaipur 302017, Rajasthan, India; hrishikeshk.ch.21@nitj.ac.in

³ Dr. B.R. Ambedkar National Institute of Technology Jalandhar, Jalandhar 144011, Punjab, India

⁴ Federal State Budgetary Scientific Institution "Federal Scientific Agroengineering Center VIM", 1st Institutskiy Proezd, 5, 109428 Moscow, Russia; kovalev_an@mail.ru (A.A.K.); vadimbolshev@gmail.com (V.B.); kovalev_ana@mail.ru (D.A.K.)

⁵ College of Agriculture, Central Agricultural University, Imphal 795004, Manipur, India; sarangi77@yahoo.co.in

⁶ Department of Plant Breeding, Swedish University of Agricultural Sciences, Alnarp, 23053 Uppsala, Sweden; aakash.chawade@slu.se

⁷ Department of Biotechnology, Dr. Ambedkar Institute of Technology for Handicapped, Kanpur 208024, Uttar Pradesh, India; msr@aith.ac.in

⁸ Russian University of Transport, 127994 Moscow, Russia

* Correspondence: vivekanand.cee@mnit.ac.in (V.V.); pancheska@mail.ru (V.P.)

Abstract: Gasification technology often requires the use of modeling approaches to incorporate several intermediate reactions in a complex nature. These traditional models are occasionally impractical and often challenging to bring reliable relations between performing parameters. Hence, this study outlined the solutions to overcome the challenges in modeling approaches. The use of machine learning (ML) methods is essential and a promising integration to add intelligent retrieval to traditional modeling approaches of gasification technology. Regarding this, this study charted applied ML-based artificial intelligence in the field of gasification research. This study includes a summary of applied ML algorithms, including neural network, support vector, decision tree, random forest, and gradient boosting, and their performance evaluations for gasification technologies.

Keywords: gasification technology; machine learning; biomass gasification; energy; applications



Citation: Meena, M.; Kumar, H.; Chaturvedi, N.D.; Kovalev, A.A.; Bolshev, V.; Kovalev, D.A.; Sarangi, P.K.; Chawade, A.; Rajput, M.S.; Vivekanand, V.; et al. Biomass Gasification and Applied Intelligent Retrieval in Modeling. *Energies* **2023**, *16*, 6524. <https://doi.org/10.3390/en16186524>

Academic Editor: Xiangpeng Gao

Received: 16 August 2023

Revised: 5 September 2023

Accepted: 7 September 2023

Published: 10 September 2023



Copyright: © 2023 by the authors. Licensee MDPI, Basel, Switzerland. This article is an open access article distributed under the terms and conditions of the Creative Commons Attribution (CC BY) license (<https://creativecommons.org/licenses/by/4.0/>).

1. Introduction

Biomass gasification is becoming increasingly popular in industrial and commercial settings for various reasons, including energy and sustainable goals [1]. It is a thermochemical process to create gaseous or liquid intermediate products that can be converted into more valuable energy (transportation fuels, electricity, etc.). The thermochemical conversion technique uses a variety of processes, including pyrolysis, torrefaction, gasification, liquefaction, and combustion (as shown in Figure 1). For companies and researchers, the simulation and optimization of the thermochemical process are extremely significant [2]. Gasification processes are complex and include several intermediate reactions that occur simultaneously at different times. This complexity requires the use of various modeling approaches, such as thermodynamic and kinetic models and process modeling, to describe a process and the influence of process parameters on energy production. Different kinds of models, such as computational fluid dynamics (CFD) [3], kinetic modeling [4], thermodynamic equilibrium [5], and artificial intelligence (AI)-based machine learning (ML) models [6], have been developed to design a more efficient gasification process.

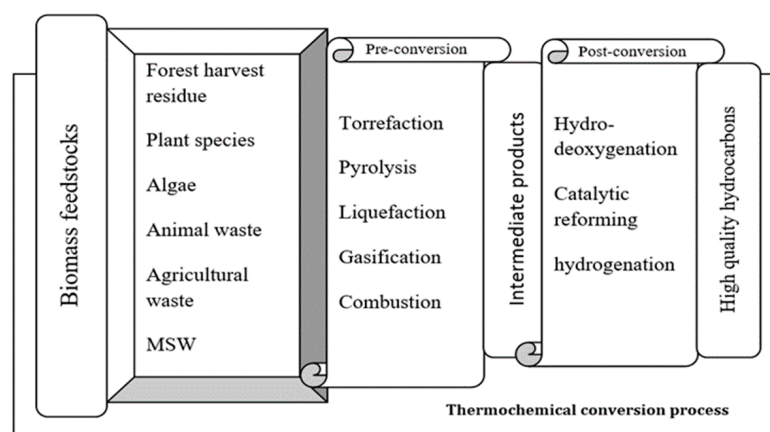


Figure 1. Thermochemical conversion processes.

Traditional modeling techniques are sometimes impractical and challenging to model uncertain relationships between parameters [7]. Therefore, developing a robust and fast modeling approach to associate the complexity of the gasification process is requisite. To overcome these issues, in the recent past, artificial neural networks (ANNs) and ML have been widely presented for the process design and optimization of gasification systems [6]. For instance, the ANN-based extreme learning model has been proposed for use in predicting SO_2 emissions [8], data-driven modeling for the gasification process [9], multivariate regression, and fluidized-bed gasifiers [10]. These techniques have been successfully applied in many fields of gasification, such as combustion optimization [11], biomass pyrolysis [12], parameter optimization [13], and catalyst screening [14]. In conclusion, the above-mentioned studies demonstrate that ML-based techniques may expand to become a more generic model to adequately forecast crucial factors and their effect on process output. These techniques are well established; however, the consideration of uncertain situations is requisite in future modeling to create the best ML-based gasification systems [15].

The provided literature studies indicate the integration of ML modeling in traditional approaches. However, the application of ML approaches in predicting the operating inputs for product outcomes often may not be very easy because, at the same time, various parameters can be influenced by multi-input features [8]. For example, the H_2 composition in syngas composition can be influenced by many parameters such as steam-to-biomass ratio, biomass composition, and equivalence ratio. Thus, developing ML models with an appropriate tactic is needed to attain high accuracy. Therefore, this study first describes the basic fundamentals of the gasification process and the various ML models that have been applied in the gasification process, followed by various evaluation techniques to validate the reliability of the developed models. Later, in Section 5, this study presents the developed studies for advanced gasification technologies in the recent past.

2. Gasification Process

Gasification is a thermochemical process that converts solid and liquid fuels such as coal, biomass, and waste lubricating oil, among, others into high-heat energy or syngas. It is a second-generation method for utilizing biomass and trash that was developed in the 18th century to produce town gas for lighting and cooking. Further, it has been utilized to manufacture transportation fuels since the 1920s. Gasification is an attractive method to generate harmless energy, with many advantages for cooking, heating, electricity generation, biofuel production, and chemical synthesis [16]. Gasification offers numerous benefits, as a variety of low- and high-value-added feedstock can be utilized in the gasification process, and biomass can be a better option for gasification in place of coal. Biomass is more reactive and has a greater volatile content, which allows the production of syngas at a lower temperature. Majorly, syngas is a composition of many gases such as H_2 , CO , CH_4 , and other hydrocarbons (Figure 2). Impurities such as tar, SO_2 , NO_2 , and NH_3 are commonly

found in gasification products [17]. Due to the impurities in gas products, the cleaning is a very important process, and catalytic hot gas cleaning is a promising technology for completely removing tar during the gasification process [18].

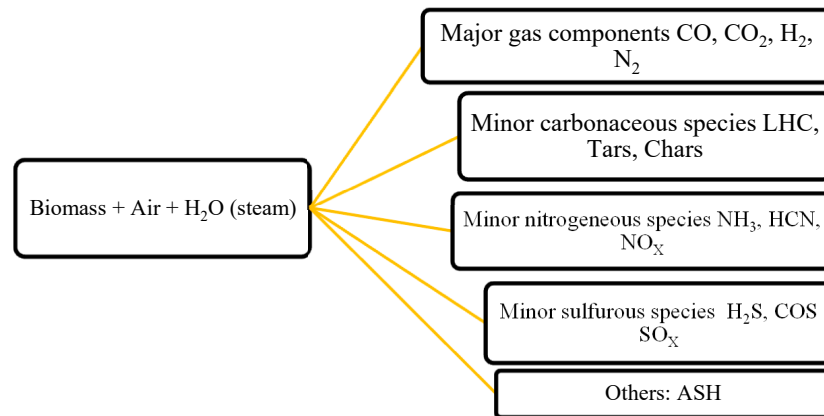


Figure 2. Gasification byproducts.

2.1. Basic Steps of Gasification Process

The gasification process occurs in four process steps, such as drying, pyrolysis, combustion, and reduction, as shown in Figure 3.

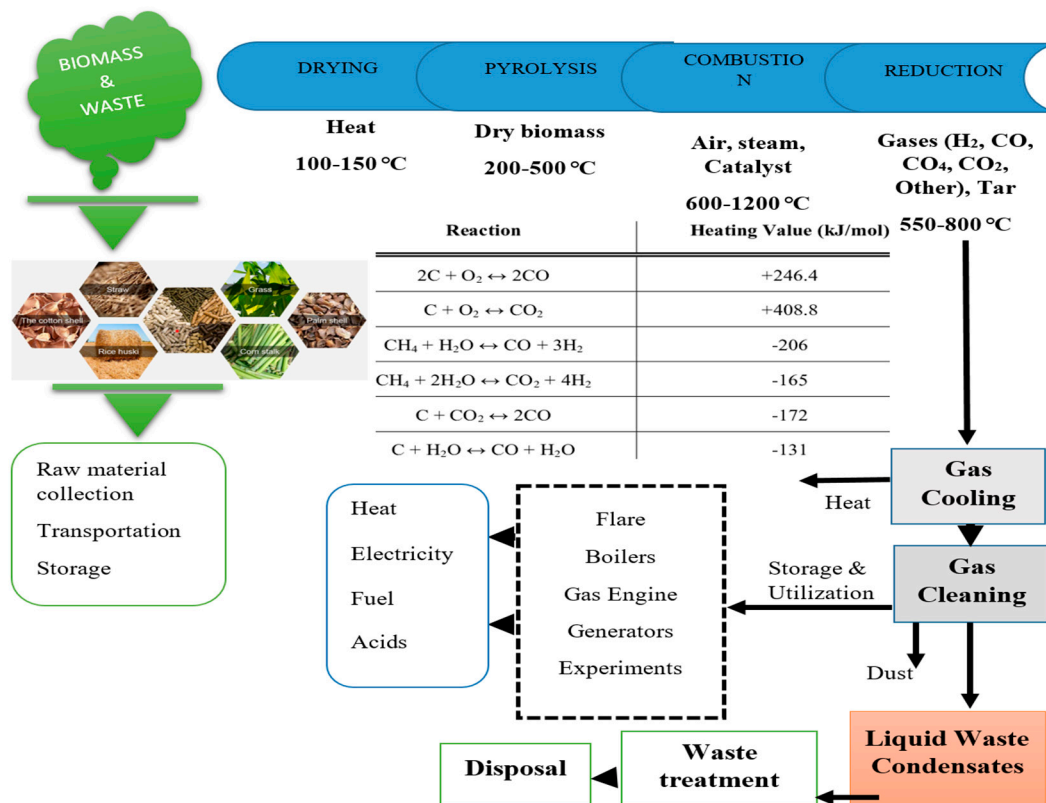
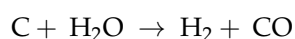
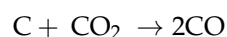
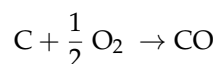
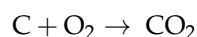


Figure 3. Various processes during gasification process.

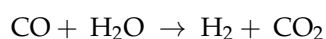
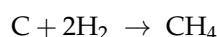
I. Drying: In this step, heat is provided to the feedstock up to a significant temperature to reduce the moisture content in the given feedstock. The higher moisture content requires high energy to make it dry, so a prior drying process is necessary as a pretreatment of the feedstock before the gasification process. Naturally dried biomass may be an ideal feedstock for the gasification process [19]. It is a sophisticated process that entails simultaneous heat and mass transportation,

as well as physicochemical changes. Heat can be transferred by direct (convection), radiant (radiation), and indirect (conduction) processes to the feedstock for drying purposes.

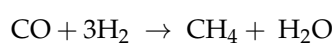
- II. **Pyrolysis:** Pyrolysis is the rapid thermal degradation of the carbonaceous material under an inert environment at high temperatures. Pyrolysis is the process of heating raw biomass, where heat is provided to the feedstock in the absence of oxygen, to break it into volatile gases and charcoal [20]. Pyrolysis is the initial phase of gasification or combustion, in which the biomass material begins to decompose with heat and breaks down into a combination of solids, liquids, and gases. While some hydrocarbons such as H₂, CH₄, and light carbon vapor (CO and CO₂) are released into gaseous forms, high temperature leads to the thermal cracking process and releases condensable compounds such as topping atmospheric residue in vapor form and solid material into the pyrolysis process, known as char material. Pyrolysis has an essential role in gasification because it can improve the syngas output and, especially, hydrogen production [21].
- III. **Combustion:** Combustion is a process known as the direct burning of biomass at high temperatures with a limited amount of oxygen in a controlled manner to generate oxidized carbonaceous feedstock. Generally, atmospheric oxygen is used as an oxidant for the combustion process [22]. During the combustion process, various gases are produced from the biomass material in the form of smoke. Combustion is the only net exothermic process in all the processes of gasification and generates heat for the other processes of drying, pyrolysis, and reduction either directly, or it can be recovered indirectly from combustion by heat exchange processes in a gasifier [23]. In the combustion process, the carbon content reacts with oxygen and starts to convert into volatile products such as carbon dioxide, carbon monoxide, and char particles. The combustion process releases a large amount of heat and energy that can be used for subsequent gasification reactions, such as



There are two basic phase-shift reactions that occur during the combustion process for the natural generation of hydrogen and methane, which are the water–gas-shift reaction and methanation. The water–gas-shift reaction in the gasifier quickly approaches equilibrium at medium temperatures, balancing the composition amounts of carbon monoxide, steam, carbon dioxide, and hydrogen.



Later, the CO and residual H₂ start to react to form methane and watering waste.



- IV. **Reduction:** Reduction is a process to completely remove the oxygen from combusted hydrocarbons to restore them to a state where they may burn again. In reduction, heat is continuously provided to raw carbon to attract oxygen from water vapor and carbon dioxide, and it is redistributed into many single-bond sites. Now, no free oxygen can survive in its diatomic state because single-bond oxygen atoms are more

attractive than the C bond. When all available oxygen is reallocated as single atoms, the reduction process is complete. In this process, oxygen atoms from CO₂ will be reduced to make two CO molecules, whereas oxygen from H₂O is also removed to produce H₂ and CO. Both H₂ and CO are combustible fuel gases that may be piped out to perform desired tasks elsewhere [24]. After the overall process, a cleaning process is required to provide efficient fuel. The cleaning of produced gas is also an important step in providing highly efficient fuel, which is a complex method after the gasification process [25].

2.2. Parameters of Gasification Process

Gas production in the gasification process depends on various parameters, such as the kind of feed material, gasifying agent, and catalyst and operating conditions, which can affect the output products [26]. Thus, the pace of reaction, conversion rate, and quality of gas output in gasification can be affected by various parameters, as shown in Table 1.

Table 1. Effect of parameters on syngas production in gasification process, adopted from [27,28].

Parameter	Observation				
	CO	H ₂	CO ₂	CH ₄	N ₂
Equivalence ratio ↑	↓	↓	↑	↓	↑
Moisture content ↑	↓	↑	↑	↑	↓
Temperature ↑	↑	↑	↓	-	-
Steam-to-biomass ratio	↓	↑	↑	↑	↓
Pressure ↑	↓	↑	↑	↑	-
CaO	↓	↑	↓	↑	-
Dolomite	↑	↑	↑	-	-
Air and oxygen	↑	↑	↑	↓	↓
CO ₂	↑	↑	↑	↑	↓
Biomass type	Normally, a material with a higher (hemicellulose þ cellulose)/lignin ratio can provide a higher syngas yield.				
Moisture content	1. Moisture content $\propto \frac{1}{\text{energy efficiency and syngas quality}}$ 2. The higher moisture leads to a decrease in temperature. The optimal moisture content is in the range of 10–20% for gasification, which can make bed temperatures more stable. However, updraft gasifiers can operate at 60% and downdraft at 25%, and plasma and supercritical reactors can operate at a high moisture content of biomass.				
Ash content	Ash content should be lower than 2% for better results.				
Particle size	1. The small size of biomass increases the surface area and diffusion resistance, improving heat transfer and enhancing gasification. Generally, a particle size between 0.15 and 51 mm is recommended for gasification. 2. A particle size smaller than 0.15 mm is recommended for entrained-flow gasifiers, >6 mm for bubbling-bed reactors, and fixed-bed reactors can tolerate >51 mm 3. The effect of particle size is reduced with temperature.				
Bed material	Bed material is inert and active. It is an energy transfer medium in gasification and can improve syngas quality and promote gas reforming and tar cracking.				
Catalysts	1. In the gasification process, the use of a catalyst can increase the surface area of the raw material and also increase the reaction rate of the process. 2. The catalyst in the gasification process is generally used to reduce the operating temperature and tar formation.				
Steam-to-biomass (S/B) ratio	1. The optimum S/B ratio varies in the range of 0.3–1.0 for gasification 2. The S/B capacity of gasifiers can be considered as follows: fixed-bed gasifiers > fluidized reactors > entrained-flow gasifiers. 3. A surplus of steam can decrease the gasification temperature and, as a result, lead to tar formation.				
Gasifying agents	Gasification agents such as air, O ₂ , steam, CO ₂ , etc., can affect syngas quality, However, external heat is required during gasification.				
Equivalence ratio	1. The optimal equivalence ratio is between 0.2 and 0.3 for fixed-bed and fluidized-bed gasifiers, and entrained-flow gasifiers usually require a 20% equivalence ratio. 2. A high equivalence ratio can promote the tar cracking process. 3. The equivalence ratio can be affected by moisture and volatile contents.				

2.3. Role of Different Gasifying Agents in the Gasification Process

During the gasification process, several gasifying agents, such as air, steam, oxygen, carbon dioxide, etc., can be used to provide higher heating values of syngas. Mostly, air is a widely useful gasifying agent because it is a cheap and highly available agent. The reaction and reactor structure are also simple for the gasification process while using air [29]. When steam and CO₂ gasifying agents are used in the gasification process, all reactions behave endothermically, and external heating is required for the gasification process. With air and oxygen, the overall reactions may be endothermic or exothermic, and the gasification process can be controlled by variations in the air or oxygen flow rates. Higher gasification temperatures are required with higher air or oxygen content [30].

Air contains a high volumetric content of nitrogen, about 79%, and this improves the nitrogen content in gasification products. Here, the HHV of syngas is significantly diluted by nitrogen, and as a result, the air gasification of biomass generally has a lower cold gasification efficiency (GCSE) that varies with the gasification temperature [31]. In the comparison of air gasifying agents, oxygen contains no or less nitrogen, and it improves the combustion process of biomass feedstock, which helps to convert more char particles into syngas or combustible gases and produces more carbon monoxide in syngas composition; thus, it has a higher CGE that can vary with the oxygen equivalence ratio (OER) and gasification temperature. Similarly, steam also avoids the dilution of nitrogen. It helps to increase the hydrogen content in syngas composition, and an appropriate amount of steam content can increase the water–gas–shift reaction and methane reforming process. Consequently, the cold gasifying efficiency (CGE) of steam gasification can be significantly increased, and it can be controlled by a variation in temperature and the steam-to-biomass ratio. Generally, carbon dioxide also gives a high CGE, as it avoids nitrogen dilution and produces rich CO and hydrogen [32] in syngas composition, but sometimes, when carbon dioxide is not efficiently consumed, carbon dioxide is diluted in syngas, which leads to the LHV of syngas.

2.4. Effects of Catalysts on Gasification

The type of catalyst is a very important factor in gasification to ensure the quality of products. Catalyst directly affects the syngas composition and manipulates the percentage volume of hydrogen, carbon dioxide, methane, and carbon monoxide [33]. In the gasification process, a suitable amount and type of catalysts can assist in reducing the gas content of carbon dioxide and maximize the potential of usable gases in gaseous products, such as hydrogen, carbon monoxide, and methane [34]. Potassium, sodium, calcium, magnesium, and heavy metals catalysts are the most commonly used catalysts in the gasification process. The effect of catalysts depends on their phase behavior; the phase activity of the catalyst must be thermodynamically favored, and inactive forms/highly volatile forms of the catalyst give a stable formation, but these are detrimental because of their complex form and the non-uniform conditions of the gasifier [35]. The catalyst in the gasification process is generally used to reduce the operating temperature and tar formation, which can be added through a precursor and exist naturally with the feed. In the gasification process, the use of a catalyst can increase the surface area of the raw material and also increase the reaction rate of the process [36].

Potassium can rapidly spread with carbonaceous materials and increase the mobility of the carbonaceous material, which increases the surface area of the material and the reaction rate of the process. The intercalation of potassium, particularly within graphitic carbon compounds, can help to enhance gasification because intercalation can increase the porosity and exposed surface area. The high volatility of potassium is a major problem with potassium catalysis that leads to the corrosion, toxic vapors, slagging, and fouling of gasifiers [37]. Similarly, as potassium, sodium is mobile and is generally a less active catalyst than potassium for gasification, but in water-soluble forms, it is the most active material like NaOH [38], Na₂CO₃ [39], or NaCl [40]. These forms also tend to be the most volatile. The sodium catalyst intercalates into the carbon structure, improves the water–gas–

shift reaction and tar cracking process, and helps in the degradation of the complex carbon structure. It is more susceptible to the gasification reaction. The use of sodium as a catalyst also has some drawbacks. Sometimes, catalyst loss may happen due to evaporation, and sodium is less volatile at temperatures above 800 °C, where it can react with water minerals and form inactive sodium aluminosilicate [41].

Another catalyst is calcium, which is not as active as alkali metals, has lower mobility, and can lead to similar initial rates of reaction as alkali catalysts. The activity of calcium catalysts decreases with the increase in the conversion rate of the carbonaceous material. The advantage of a calcium catalyst is that it can help to reduce CO₂ levels in the gasification process, as CO₂ cannot be further oxidized, and as a result, this improves the heating value of the produced syngas. In the form of CaO, it can adsorb CO₂ from the generated syngas and form CaCO₃, which increases the concentration of H₂ and CO in the syngas and reduces the requirement for downstream processing [42]. Moreover, calcium can also absorb sulfur and limit the formation of toxic elements, promoting inert nitrogen during gasification. The slugging and obstruction of feed flow into reactors are major disadvantages of calcium catalysis in gasification. Like calcium, magnesium is also a less active earth-alkaline metal catalyst. Dolomite, which is a combination of calcium and magnesium, is the most suitable type of magnesium as a catalyst. Increases in the Ca/Mg ratio, where calcium is the predominant catalytic species in dolomite, can boost the activity of dolomite catalysts. Magnesium shows similar catalysis activities to calcium, including low volatility and eutectic formation with other metals. Due to low catalytic activity, dolomite and olivine are the most useful materials in the fluidized-bed gasification process [43].

Iron, nickel, and some heavy metals can be used as gasification catalysts. These can be found in carbon sources naturally and obtained cheaply as waste catalysts from other processes. Iron encourages the production of wider pores than sodium or potassium and creates less surface area. Iron also behaves like calcium, as it converts H₂S to non-toxic compounds, but the major drawback is that it is less active and converts nitrogen into toxic elements such as HCN or NO₂ [44]. Furthermore, nickel is also an active material catalyst for gasification that can increase the hydrogen and methane composition in the product. Like iron, nickel is also able to convert sulfur compounds into the vapor phase during gasification, as it forms Ni₃S₂ with a sulfur compound. The Ni/ZrO₂ catalyst can also help to increase steam reforming and pyrolysis while inhibiting polymerization and aromatization processes [45]. The major issue with the use of nickel as a catalyst is that it cannot absorb CO₂. Nickel is mostly employed with microalgae and liquid feeds to gas reforming after gasification. Copper and Ru are other heavy metals that can perform better than potassium in the gasification of slurries at low temperatures around 400 °C. Additionally, ruthenium can also improve the formation of H₂ and CH₄ [46].

2.5. Fuel Characteristics

The real identification of a good gasifier is not only dependent on its fuel conversion ability. The qualities of the generated gas must also be assessed. There is no such thing as a universal gasifier. Each gasifier is designed to provide a specific fuel quality [47]. The characteristics of fuel can be used to classify a gasifier fuel's reliability. The moisture content in combustible fuel always depends on the type of raw material and its origin. Low moisture content is necessary for a reliable fuel because there will be significant heat loss from evaporation. High moisture content in biomass material not only reduces the heat budget but also increases the load on cooling and filtration equipment. Some pretreatment of fuel is necessary to lower the moisture content. Fuel moisture content should be less than 20% in general [48]. All gasifier fuels produce dust, which can block the internal combustion engine, so it needs to be removed, and the ideal gasifier should not produce more than 2–6 g/m³ of dust [49]. The more dust created, the greater the burden on filters, meaning regular cleaning and maintenance service. Tar is the most unwanted component of gasoline because it tends to build up around the carburetor and intake valves, creating sticking and inconvenient operation. It can vary in color, from brown and watery (where

it contains 60 percent water) to black and viscous (where it contains 7 percent water), depending on temperature and heat rate. So far, over 200 chemical components have been discovered in tar [50]. The majority of efforts have gone towards filtering and cooling this tar. A well-designed gasifier should produce tar at a rate of less than 1 g/m^3 and a low-heating-value fuel in the range of $1000\text{--}1200 \text{ kcal/m}^3$ [51].

3. Artificial Intelligence in Biomass Gasification

ML-based AI is a reliable integration to conventional models in the gasification process to correlate the complexity of the process. These techniques can assist the design of processes with higher carbon conversion efficiency to reduce the process time and costs of complex and time-consuming practices [52]. These techniques have been widely applied in gasification processes for various purposes, such as to study the reaction mechanism of conversion processes and design computational algorithms to achieve a desired task [53]. Several studies featuring ML in the gasification process have been developed by researchers to forecast and manage the process with largely reliable outcomes during decision making. The research methodology to develop a robust and more accurate ML-based model can be understood as that in Figure 4. To develop a model, it is first required to collect the data from various preprocessing steps or modeling, i.e., ASPEN and other simulation tools. Then, later, the use of ML models can help to learn the correlation between variables of experimental data without detailed knowledge or expert experience of the process, which is more flexible and low cost in practice, thus achieving great attention. Regarding this, various ML-based AI modeling approaches for process development are highlighted in this section. For a better understanding of these models, kindly see the reference studies.

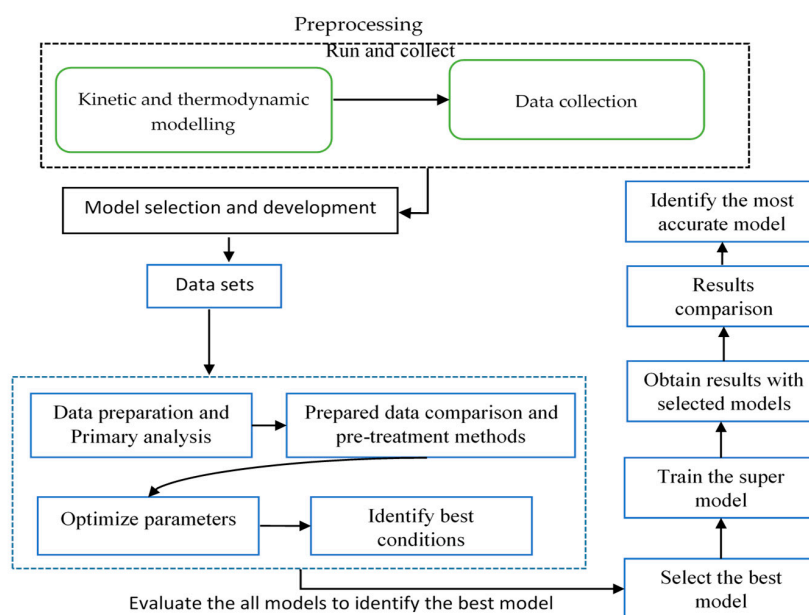


Figure 4. Methodology to identify appropriate ML model, adopted from [54].

3.1. Artificial Neural Network (ANN)

The artificial neural network (ANN) is one of the most advanced ML techniques for identifying complicated correlations between input and output data. It is a mathematical model inspired by the principle of biological neurons to solve difficult problems [55]. The ANN is an attractive ML method for applications involving prediction due to its distinctive features. ANN models are flexible enough to incorporate linear and non-linear input–output mappings. A neural network model generally includes input, hidden, and output layers, where each layer can contain multiple neurons and be formulated as in Equations (1) and (2). During the solution, in an ANN model, the input signal has to be transmitted from the input layer to the output layer through various hidden layers with

the help of the activation function, bias vector, and weight. Nowadays, ANN technology has been successfully applied in the gasification process for various purposes, such as parameter prediction in gasifiers [56], material analysis [57], efficiency evaluation [58], and economic and environmental analyses [59]. For the gasification process, the material contents, such as carbon, hydrogen, oxygen, moisture content, ash, volatile materials, etc., can be used as input variables, while gas outputs, heating values, emissions, and wastes and economics can be output variables.

$$H_{ij} = f\left(\sum_{i=1}^I X_{0i}W_{0i,j} + B_0\right) \tag{1}$$

$$Y_t = f\left(\sum_{j=1}^J H_{mj}W_{mj,t} + B_{Hm}\right) \tag{2}$$

where I , J , and T signify the number of neurons in the input, hidden, and output layers, respectively; f is the activation function; m refers to the number of hidden layers; and B and W stand for the threshold and weight values.

3.2. Physics-Informed Neural Network

A critical challenge for ML in applications is its physical interpretability, which can play an essential role in understanding the mechanisms behind a complex system and reduce the capability of industrial design for optimal system performance. Therefore, in the context of gasification, a physics-informed neural network (PINN) is developed in [60] to predict syngas products, which simultaneously considers regression, structure, and physical monotonicity constraints in the loss function to provide physically feasible predictions, as shown in Equation (3):

$$E = E_r + \lambda_s E_s + \lambda_p E_p$$

$$E = \sum_{i=1}^N \left(o^{(i)} - t^{(i)}\right)^2 + \lambda_s \left\{ \sum_{j=1}^n \sum_{k=1}^{\tilde{N}} \left(w_{jk}\right)^2 + \sum_{k=1}^{\tilde{N}} \left(\beta_k\right)^2 \right\} + \lambda_p \left\{ \sum_{j=1}^n \sum_{i=1}^{T_j} \frac{1 - m_j^{(i)} \times \text{sign}\left(\frac{\partial o}{\partial x_j}\left(x_{\text{syn}}^{(i)}\right)\right)}{2} \right\} \tag{3}$$

where E_r represents regression loss, E_s is structural loss and E_p stands for physical loss. The PINN model has shown outperformed prediction capability ($R^2 = 0.95\text{--}0.97$) in maintaining the correct monotonicity in feedstock characterization [60].

3.3. Multiple Linear Regression (MLR)

The variables in the gasification process can be more effective in predicting the dependent variable by the optimizing combination of multiple independent variables. The MLR model can provide the fitting to the dataset while interpreting the relationship between two or more variables [61]. It can be formulated as in Equation (4):

$$y_i = m + \alpha_1 x_1 + \alpha_2 x_2 + \dots + \alpha_i x_i + \phi \tag{4}$$

where y_i is the predicted value, $\alpha_i x_i$ refers to the regression coefficient of the i th independent variable, m is the intercept, and ϕ is the model error. In [61], an MLR model was developed for three inputs: X_1 (pyrolysis temperature), X_2 (combustion), and X_3 (equivalence ratio) with other output variables: gas yield (Y_1), residue (Y_2), tar yield (Y_3), H_2 (Y_4), CO (Y_5), CO_2 (Y_6), and CH_4 (Y_7). The mentioned study also shows the usability of ML models in the gasification process.

3.4. Support Vector Machine (SVM)

The SVM model is used for problems relating to unknown objects with a fixed number of possibilities. Its decision boundary maximizes the target hyperplane for learning samples, which can turn the problem into a convex quadratic programming problem [62]. In SVM, an experimental dataset with specific inputs (x_i) is used to predict a specific response

or target value (y_i). This robust machine learning algorithm can perform both classification and regression in linear and non-linear problems with minimal risk [63]. It can employ different non-linear mapping functions such as sigmoid, polynomials, and radial basis functions (RBFs) for solving problems. Unlike traditional regression techniques (for example, polynomial fitting), support vector machine regression (SVR) is a non-parametric regression model in which the regression hyperplane is determined to improve the capability of the SVM by optimizing the distance of nearby data points [64]. Further, Figure 4 describes the use of support vectors to develop a hyperplane. It should be noted that the support vectors indicate data points from either class that are nearest to the hyperplane. Support vector regression (SVR) can be obtained by extending the SVM from the classification problem to the regression problem. Its regression function is expressed in Equation (5). The relevant derivation procedures can be found in the work [65].

$$f(x, \alpha_i, \alpha_i^*) = \sum_{i=1}^N (\alpha_i^* - \alpha_i) (X_i^T X) + b \quad (5)$$

in which $X_i^T X = \phi(x)$, where $\phi(x)$ is the kernel function, α , α^* are Lagrange multipliers, and N is the number of observations.

Different from most ML models, SVM models can achieve better predictions without the use of hidden layers. They can significantly improve the model's flexibility by using various kernel functions with different polynomial functions.

3.5. Decision Tree

The decision tree (DT) method is widely applied in spatial data mining, known as a tree structure, which can be a binary tree or a non-binary tree. The DT model represents a mapping relationship between object attributes and object values. The DT method consists of three basic parts: decision nodes (which aid in feature storage), decision links (which aid in criteria selection), and decision leaves (which aid in classification). In this, each non-leaf node represents a test on a feature attribute, each branch represents the output of the feature attribute in a given range, and each leaf node stores a category of solutions [66]. A path from the root to the leaves stands for the value of input parameters and each leaf indicates the value of targeted parameters. To establish the DT model for the gasification process, it is required to describe the input and output vectors as X and Y distributions, respectively. Further, a trained dataset (D) in the DT can be obtained using Equation (6). After that, the input space can be divided into m units, and the DT model can be written as shown in Equation (7):

$$D = \{(x_1, y_1), (x_2, y_2), \dots, (X_N, Y_N)\} \quad (6)$$

$$f(x) = \sum_{m=1}^M C_m I(x \in R_m) \quad (7)$$

where n signifies the number of features, N indicates the sample size, and C_m refers to the fixed output value for the m th unit.

3.6. Random Forest

Random forest (RF) is an evolved version of the DT algorithm. Rather than utilizing a single huge DT, various DTs can make an RF learning algorithm to overcome the challenges of the overfitting of the DT [66]. In the RF algorithm, a number of created DTs that have been trained with subsets of the original data are used to learn concurrently. The number of decision trees that are executed concurrently varies depending on the task and has a significant impact on the algorithm's performance. The RF regression problem can be solved using a normal binary decision tree that has many branches, a root, many nodes, and leaves. A branch is essentially a chain of nodes that extends from the root to the leaves, with each node denoting a property. To determine splitting criteria for the regression tree, a

Gini index (GI) is the best principle to judge the classification quality for RF algorithms [67].

$$Gini_{index(D(o), k^*)} = \sum \frac{|D(s)|}{|D(o)|} Gini(D(s)) \tag{8}$$

$$k^* = argmin Gini_{index(D(o), k^*)}$$

where the $D(o)$ dataset is classified into subset $D(s)$, and the GI for each subset can be evaluated by Equation (8). The GI value of subsets can show the purity of subsets, and a lower GI value suggests a higher quality of classification. k^* is an optimal attribute, and the minimum GI value based on the k^* can be selected as the result.

3.7. Gradient Boosting Algorithm

Recently, the family of gradient boosting (GB) algorithms has grown with a number of novel concepts (such as XGBoost [68], LightGBM [69], and CatBoost [70]) that place a dual emphasis on speed and accuracy. XGBoost is a modular ensemble strategy that has shown to be an effective and dependable way to handle machine learning problems. With the use of selective sampling from high-gradient examples, LightGBM is an accurate model that is dedicated to providing incredibly quick training performance. In order to increase the accuracy, CatBoost modifies the computation of gradients to prevent prediction shifts [71]. GB is an additive weighted-sum approximation of function $F^*(x)$

$$F_m(x) = F_{m-1}(x) + \rho_m h_m(x), \tag{9}$$

where ρ_m is the weight of m th function, and these functions are ensembles as DTs. This additive approximation is constructed iteratively. First, it is required to determine a constant approximation of $F^*(x)$, as in Equation (10):

$$F_0(x) = arg \min_{\alpha} \sum_{i=1}^N L(y_i, \alpha). \tag{10}$$

Further, subsequent models are required to minimize, as in Equation (11):

$$(\rho_m, h_m(x)) = arg \min_{\rho, h} \sum_{i=1}^N L(y_i, F_{m-1}(x_i) + \rho h(x_i)) \tag{11}$$

Now, instead of solving the optimization problem, here, each h_m can be treat as a greedy step for $F^*(x)$. For that, each model is required to be trained with different h_m of new datasets $D = \{x_i, r_{mi}\}_{i=1}^N$, and the pseudo-residuals r_{mi} can be calculated as

$$r_{mi} = \left[\frac{\partial L(y_i, F(x))}{\partial F(x)} \right]_{F(x)=F_{m-1}(x)}$$

where the value of ρ_m is consequently computed by solving a line-search algorithm.

4. Evaluation Methods

ML can be applied at the moment to make highly accurate predictive models and understand the associations between the input variables and output responses of highly non-linear processes. Since each feature contributes separately to an ML model, the correlations in numerous input characteristics helps to maintain all the properties of a model. Therefore, various techniques to determine the degree of correlation between two or more variables in ML models are included in this section.

4.1. Mean Impact Value (MIV)

The mean impact value (MIV) is mainly applied to the modification of the neural network model. It can evaluate the importance of the variables to the alternation of the weight matrix in the neural network [72]. It can help to observe the impact change of the i th independent variable on the output result, which is formulated in Equations (12) and

(13). The sign of the MIV shows the positivity and negativity of the independent variable on the dependent variable, and the absolute value indicates the degree of the independent variable’s influence on the dependent variable [73].

$$IV_i = Y_i^{(1)} - Y_i^{(2)} \tag{12}$$

$$MIV_i = \frac{1}{m} \sum_{j=1}^m IV_i(j), i = 1, 2, \dots, n \tag{13}$$

where IV_i is the change value vector by influence on the output after the changes in independent variable, Y_i is the corresponding output vector when the independent variable changes, and m is the number of observations for independent variable vectors, including n variables. Additionally, to understand the applicability of the MIV with an ML model, kindly see ref. [72].

4.2. Pearson Correlation Coefficient

The linear connection between two variables can be discovered using the Pearson coefficient technique, which is quantified in statistics as in numbers between -1 and 1 [74]. If the correlation coefficient is larger than 0 , it means a variable is increasing with another variable and showing a positive connection between them. Generally, a higher absolute value of the correlation coefficient indicates a stronger connection between these two variables. To determine the Pearson correlation coefficient for a problem, let us suppose $(X_1, X_2, X_3, \dots, X_n)$ and $(Y_1, Y_2, Y_3, \dots, Y_n)$ are n -dimensional random variables, and they have a correlation. Further, the Pearson correlation coefficient of X_i and Y_i can be defined as in Equation (14):

$$r_{xy} = \frac{N \sum_{i=1}^N x_i y_i - \sum_{i=1}^N x_i \sum_{i=1}^N y_i}{\sqrt{N \sum_{i=1}^N x_i^2 - \left(\sum_{i=1}^N x_i\right)^2} \sqrt{N \sum_{i=1}^N y_i^2 - \left(\sum_{i=1}^N y_i\right)^2}} \tag{14}$$

4.3. Shapley Additive Explanation (SHAP)

SHAP analysis has been successfully applied to biomass thermochemical conversion studies, in wastewater sludge pyrolysis [75], in the biomass microwave pyrolysis process [76], hydrothermal processing [77], and the biomass and plastic co-pyrolysis processes [78]. To quantify the feature importance [79] in ML models, the Shapley additive explanation (SHAP) algorithm has been developed in [80], which is based on the magnitude of feature attributes and can help to analyze feature importance and their effects on results. SHAP is based on the combined cooperative game theory approach, which can provide a degree of relevance to each characteristic at a given prediction along with three other parameters: local accuracy, missingness, and consistency. Further, following the definition of additive feature attribution with three properties, the SHAP value for the explanation ML model can defined as in Equation (15):

$$\varphi_i(f, x) = \sum_{z' \subseteq x' / \{i\}} \frac{|z'| (M - |z'| - 1)!}{M!} (f_x(z' \cup \{i\}) - f_x(z')) \tag{15}$$

where $|z'|$ is a subset of non-zero entries in $x' / \{i\}$, $|z'| (M - |z'| - 1)! / M!$ is the fraction of permutations with the feature $\{i\}$, and $(f_x(z' \cup \{i\}) - f_x(z'))$ is the marginal contribution of the feature $\{i\}$ to condition z' .

4.4. Regression Evaluation Methods

To assess the prediction performance of these ML models, it is required to evaluate various features, as shown in Table 2. In the evaluation indicators, a smaller value of the SSE, MSE, MAE, RMSE, MeanRE, and MaxRE for the ML models indicates the higher prediction accuracy of a model. Meanwhile, the higher the value of R^2 , the better the prediction performance [81].

Table 2. Statistics to evaluate the performance of ML models, adopted from [81–83].

Statistical Methods	Mathematical Formulation
Actual error (AE)	$ Actual - Predicted\ values $
Sum of squares error (SSE)	$\sum_{i=1}^n (y_{predict} - y_i)^2$
Standard deviation (SD)	$\sqrt{\frac{\sum(actual - mean)^2}{n}}$
Mean absolute error (MAE)	$\frac{1}{n} \sum_{i=1}^n (y_{predict} - y_i) $
Mean standard error (MSE)	$\frac{1}{n} \sum_{i=1}^n (y_{predict} - y_i)^2$
Relative absolute error (RAE)	$\frac{[\sum_{i=1}^n (Predicted - actual\ value)^2]^{1/2}}{[\sum_{i=1}^n Actual\ value^2]^{1/2}}$
Root mean square error (RMSE)	$\sqrt{\frac{1}{n} \sum_{i=1}^n (y_{predict} - y_i)^2}$
Normalized root mean squared error (NRMSE)	$\frac{RMSE}{Average\ of\ observed\ values}$
Average relative error (MeanRE)	$Mean\left(\frac{y - y_{predict}}{y} \times 100\%\right)$
Maximum relative error (MaxRE)	$Max\left(\frac{y - y_{predict}}{y} \times 100\%\right)$
Mean absolute deviation (MAD)	$\frac{1}{n} \sum_{i=1}^n Actual\ output - mean\ actual\ output $
Coefficient of determination (R^2)	$(1 - (sum\ of\ square\ errors / sum\ of\ squares))$
Adjusted coefficient of determination ($adj(R^2)$)	$1 - \left[(1 - R^2) \times \frac{n-1}{n-k-1}\right]$
Linear correlation coefficient (R_D)	$\sqrt{1 - \frac{\sum_{i=1}^n (y_{p,i} - y_{a,i})^2}{\sum_{i=1}^n (y_{a,i} - \bar{y}_a)^2}}$
Regression correlation coefficient (R_C)	$\sqrt{1 - \frac{\sum_{i=1}^n (y_{p,i} - y_{a,i})^2}{\sum_{i=1}^n (y_{a,i})^2}}$

5. Application of Artificial Intelligence in Gasification Process

The AI method has been widely used to estimate the outputs by gasification [84] in a downdraft gasifier [85], a circulating fluidized-bed gasifier [86], and a bubbling-bed gasifier [87] with good accuracy. Based on recent progress, in this section, recent AI-based gasification systems are critically reviewed. A significant amount of literature has been written in the last four years on modeling and forecasting the performance of gasification systems. The majority of these studies have examined the impact of operating parameters on performance. These applications are classified in this section.

5.1. AI in Prediction and Performance Evaluation

AI shows unique advantages in the prediction, evaluation, and optimization of gasification systems. In recent years, ML approaches for predicting biomass gasification production have been widely studied and reviewed [81]. The implementation of other ML methods, such as RF, GBR, XGB, SVM, and ANN, has been widely acknowledged in the field of biomass and waste transition. For instance, various applications of AI-based models in the context of prediction have been applied in the gasification process:

- ANN and particle swarm optimization (PSO)-based hybrid models were built to predict the product yield, which reduced the deviation of CO concentration from 13.93 to 8.39% [57].
- The GBR model is more convincing than the ANN model in predicting syngas compositions with real experimental data [88].
- A hybrid AI approach is remarkably satisfied, with a 0.134% mean prediction error to predict the hydrogen concentration in a downdraft fixed-bed gasifier [89].
- A stochastic GB (SGB) decision tree framework is proposed in [90] for modeling and quantifying the degradation kinetics of biomass, which shows high performance with a 0.993 determination coefficient.

- An AI-based hybrid model for solid fuel classification in energy harvesting from agricultural residue is discussed in [91].
- An ANN model is used to estimate the performance efficiency of a gasification system by using the back-propagation method. The study predicts the chemical exergy, and there are very few studies available in the context of chemical exergy analysis [85].
- Five different machine learning models are applied with an optimized ensemble model for predicting lower heating value (LHV) and syngas yield [80].
- Moreover, another study shows that the Gaussian-type kernel with a least-squares SVM can provide the best monitoring for biochar prediction [92].

5.2. Design of Integrated Gasification Systems

There are numerous research studies on integrated gasification systems, as highlighted in [93]. A study focused on the modeling of a solid-oxide fuel cell (SOFC), which utilized three integrated processes including gasification to achieve the most optimal system from the perspective of energy and economics [94]. Further, in another research direction, the Aspen Plus simulator was used to develop a circulating fluidized bed (CFB)-based fuel-cell-integrated system. Thereafter, the created data set was utilized to train the artificial neural network (ANN) model and examine the impacts of different torrefied biomass samples on PEM fuel cell outputs for a sophisticated integrated system [95]. Additionally, based on the multi-level factorial and design of experiment methodology, a configuration of the tri-generation process such as valorization, gasification, and solid-oxide fuel cell (SOFC), is discussed in [96]. Moreover, a configuration for the hybridization of geothermal and biomass energies is analyzed in [97], in which geothermal heat is employed for water heating and steam generation. In order to assess the feasibility of the proposed systems and to compare their performance, detailed simulation models are made based on the first and second laws.

5.3. In Gasification of Municipal Solid Waste

When municipal solid waste (MSW) is not properly managed, it can cause severe health and environmental problems by polluting the air, water, and soil. Due to its porous nature and the non-linear relationships between different factors, the modeling and simulation of the gasification process of MSW is difficult and computationally complex. Regarding this, an ML model is developed in [20] for MSW gasification, but despite its prediction capability, the developed model undergoes several deficits, such as the consideration of catalyst properties. Thus, this study is devoted to creating an inclusive ML model to understand the non-catalytic MSW gasification process. Further, three ML approaches, SVM, RF, and GBR, are applied to characterize the MSW gasification process for parameter identification. In addition, SHAP analysis is also used to attain the best-performing responses in the modeling process [80]. Furthermore, recently, five sophisticated soft computing models, DT, XGB, RF, MLP, and SVR, have been developed to analyze the performance of MSW gasification in fluidized-bed gasifiers [98]. These five models are optimized using the PSO technique. As a result, the heating value of gas (LHV), the heating value of gasification products (LHVp), and the syngas production in the process of MSW gasification can all be predicted by using the developed model.

5.4. For Environment Protection and Performance Analysis

For the prediction of environment-affecting parameters of gasification, Ref. [99] highlights the experiences of environmental modeling. In addition, in a study, a genetic-algorithm-based AI model is proposed to minimize the CO₂ emission in the process of anaerobic digestion [100]. Further, ANN and TOPSIS techniques are used in the multi-criteria optimization of three distinct subsystems (heating, cooling, and electricity) to determine the optimal point for high energy efficiency and less CO₂ emission in the gasification process [58].

In the context of performance analysis, the use of thermogravimetric analysis to determine the mass loss in the gasification environment is a potential method for comprehending the chemical reactions, reactivates, and kinetic characteristics of the gasification material [101]. Additionally, according to [102], the genetic-algorithm-based ML model has shown the best performance in polygeneration systems to effectively evaluate the access of power, heat, freshwater, and hydrogen generation using biomass and solar energy. The extra heat in output gases can be employed to boost the desalination system's ability to perform reverse osmosis to raise the steam water's intake pressure [103].

Accordingly, during the literature review, AI showed unique advantages in the prediction, evaluation, and optimization of gasification systems, which is promising and attractive. Based on recent progress, this article summarizes several critical AI-based technologies for the future development of gasification systems. Additionally, various applications of AI in gasification systems are included in Table 3.

Table 3. AI-based applied technologies in gasification process.

Work	Errors/Accuracy	Research Area	Refs.
Linear regression and SVM applied in updraft gasifier	$R^2 \approx 0.99$, $0.008 < MSE < 2.66$	SVM classification	[75]
Automated sludge pyrolysis	$R^2 \geq 0.813$, $RMSE \leq 12.51$	RF, regression	[104]
Co-gasification of coal–biomass blend	Exergy = 34.19%	HHV prediction	[105]
Environmental impact of palm kernel shell	Improved to 65.44 vol%	Steam gasification, Cao sorbent	[106]
Experimental and AI-based study on catalytic reforming during pyrolysis		Structure modeling, pyrolysis	[107]
Emission control in reactors		Chemical looping	[108]
ML algorithms to determine heat capacity	$R2 = 0.99347$	Oil reservoir	[109]
Emission control in anaerobic digestion	Emission = 36.3%	H2 production	[100]
GB-based electrochemical and thermal tri-generation process	Exergy efficiency = 34.6%	Multi-objective optimization	[110]
Back-propagation (BP) neural network for microwave-assisted cracking	Efficiency = 95.7%	Catalytic pyrolysis	[111]
Prediction of torrefaction severity index	Mean error = 0.9784	Adaptive regression	[112]
Economically feasible design of wind turbine integrated gasification process	Exergy increased by 7.3%	Thermodynamic analysis,	[113]
100-year scaling of fluidized-bed and circulating fluidized-bed reactor.		fouling mitigation, clustering	[114]
Multi-objective optimization for flash cycling of SOFC system	Exegetic efficiency = 53.23%	Performance analysis	[115]

6. Future Research Directions

With the advantage of ML modeling, gasification is becoming a promising technology. However, the incorporation of various research methodologies into the gasification process may be a required step to develop more accurate and robust systems.

6.1. Uncertainty in Machine Learning

In ML modeling, statistics are crucial in understanding the relevance between the input and output features [80]. This “underestimation” or “misunderstanding” increases the uncertainty in research to evaluate algorithms. Therefore, it is noteworthy to explain the types of uncertainty corresponding to the machine learning algorithm. In ML modeling, there are three factors where uncertainty can arise: (1) noise in the collected datasets; (2) prediction range; and (3) valid model selection [44]. Further, to manage these uncertainties, several optimization techniques can be used. The standard way to perform uncertainty analysis in most modeling practices is to perform a simple sensitivity analysis. However, in the context of managing uncertainties, there are many optimization techniques that can be applied to manage uncertainties, such as stochastic optimization [116] and robust optimization [117]. In all, robust optimization has gained a lot of attention in the past decade.

6.2. Data-Driven Approaches to Manage Uncertainty

Uncertainty-based data-driven ML methods can be a useful addition to address the limitations of traditional modeling methods for better prediction and accuracy in the gasification process. Recently, in Ref. [83], various applications of data-driven ML methods to biodiesel research were reviewed, with the conclusion that data-driven ML methods have proven superior in the modeling of complex chemical processes as compared to traditional methods. The data-driven approach to creating an uncertainty set is practically the preferred choice when no prior knowledge of the uncertainty distribution is available. In addition, data-driven uncertainty sets can be developed by using a variety of statistical and analytical methodologies, including data-driven chance-constrained programs [118], data-driven RO [119], forward and backward deviation [120], kernel density estimation [121], and kernel support vector clustering [122], which can help to improve the performance of ML models.

6.3. Response Surface Methodology as ML Techniques

Most studies in the field of response surface methodology (RSM) have focused on its application for multi-objective optimization. Recently, a study evaluated the performance of RSM as an ML technique in the gasification process [123], where the high validity of root mean square errors was evaluated at 0.235, 0.438, 0.294, and 1.999. Therefore, in the future, the design of gasification parameters by using the RSM can be a valuable approach.

6.4. Hybrid Machine Learning Models

The broader energy industry has shown enormous potential for the hybridization of ML models with other ML approaches or cutting-edge statistical methodologies. Researchers have also considered hybrid models to simulate thermochemical processes more recently [124]. Hybrid models often provide more accuracy and generalizability than conventional models but at the expense of an increase in computing burden. For instance, ensemble approaches with GB can transform a number of ineffective and underwhelming models into powerful ones. Therefore, an ensemble model can be an important future research direction to increase model resilience, even when there are little data available for model training, as demonstrated in recent work [98].

6.5. Automated Machine Learning

Applying an automated ML (AutoML) framework is more prevalent than trying out different ML model techniques. It is challenging, even for ML experts, to include all current best practices in their modeling [80]. Many obstacles to organizing high-performance ML models may be removed via autoML. Additionally, it only ever provides the optimal ML algorithm, which includes data splitting/processing, feature engineering, parameter modifications, and model selection procedures [125]. Several autoML frameworks, such as auto-sklearn [126], TPOT [127], Auto-WEKA [128], and AutoGluon [129], have been created throughout the years. Since AutoML was created for specialists with outstanding system performance, these frameworks are renowned for being quicker, more reliable, and significantly more accurate for the ML modeling of tabular data. Hence, these approaches can be used to better understand and explain the optimized ML results.

7. Conclusions

Biomass gasification is becoming increasingly popular in industrial and commercial settings for a variety of reasons, including sustainable goals. Gas production in the gasification process always depends on various parameters and properties of materials. Numerous modeling approaches, including computational fluid dynamics and thermodynamic and kinetic models, are frequently used to develop gasification systems. The traditional models are sometimes impractical and often challenging to bring a reliable relation between parameters. Hence, the use of ML-based AI methods is becoming a promising integration to add intelligent retrieval to traditional modeling approaches. Therefore, this study critically

reviewed the application of the AI-based approach in gasification technology. In addition, future aspects and requirements of modeling in the gasification process are also concluded.

Author Contributions: Conceptualization, methodology, writing—original draft preparation, M.M., V.V. and N.D.C.; investigation, resources, data curation, H.K., A.A.K., V.B., D.A.K., P.K.S. and V.P.; writing—review and editing, visualization, A.C. and M.S.R.; supervision, V.V. and N.D.C. All authors have read and agreed to the published version of the manuscript.

Funding: The authors thank MNIT Jaipur and IIT Patna for all their infrastructure and support.

Data Availability Statement: The useful data to support the findings of study are included within the article.

Conflicts of Interest: The authors declare no conflict of interest. The funders had no role in the design of the study; in the collection, analyses, or interpretation of data; in the writing of the manuscript; or in the decision to publish the results.

References

1. Gopalakrishnan, P. Modelling of Biomass Steam Gasification in a Bubbling Fluidized Bed Gasifier. Ph.D. Thesis, University of Canterb, Christchurch, New Zealand, 2013.
2. Chen, X.; Zhang, H.; Song, Y.; Xiao, R. Prediction of product distribution and bio-oil heating value of biomass fast pyrolysis. *Chem. Eng. Process.-Process Intensif.* **2018**, *130*, 36–42. [[CrossRef](#)]
3. Hasse, C.; Debiagi, P.; Wen, X.; Hildebrandt, K.; Vascellari, M.; Faravelli, T. Advanced modeling approaches for CFD simulations of coal combustion and gasification. *Prog. Energy Combust. Sci.* **2021**, *86*, 100938. [[CrossRef](#)]
4. Wang, Y.; Kinoshita, C.M. Kinetic model of biomass gasification. *Sol. Energy* **1993**, *51*, 19–25. [[CrossRef](#)]
5. Materazzi, M.; Lettieri, P.; Mazzei, L.; Taylor, R.; Chapman, C. Thermodynamic modelling and evaluation of a two-stage thermal process for waste gasification. *Fuel* **2013**, *108*, 356–369. [[CrossRef](#)]
6. Ayub, Y.; Hu, Y.; Ren, J. Estimation of syngas yield in hydrothermal gasification process by application of artificial intelligence models. *Renew. Energy* **2023**, *23*, 118953. [[CrossRef](#)]
7. Kushwah, A.; Reina, T.R.; Short, M. Modelling approaches for biomass gasifiers: A comprehensive overview. *Sci. Total Environ.* **2022**, *834*, 155243. [[CrossRef](#)] [[PubMed](#)]
8. Yu, H.; Gao, M.; Zhang, H.; Chen, Y. Dynamic modeling for SO₂-NO_x emission concentration of circulating fluidized bed units based on quantum genetic algorithm-Extreme learning machine. *J. Clean. Prod.* **2021**, *324*, 129170. [[CrossRef](#)]
9. Liu, S.; Hou, Z.; Yin, C. Data-driven modeling for UGI gasification processes via an enhanced genetic BP neural network with link switches. *IEEE Trans. Neural Netw. Learn. Syst.* **2015**, *27*, 2718–2729. [[CrossRef](#)]
10. Chavan, P.; Sharma, T.; Mall, B.; Rajurkar, B.; Tambe, S.; Sharma, B.; Kulkarni, B. Development of data-driven models for fluidized-bed coal gasification process. *Fuel* **2012**, *93*, 44–51. [[CrossRef](#)]
11. Kalogirou, S.A. Artificial intelligence for the modeling and control of combustion processes: A review. *Prog. Energy Combust. Sci.* **2003**, *29*, 515–566. [[CrossRef](#)]
12. Cahanap, D.R.; Mohammadpour, J.; Jalalifar, S.; Mehrjoo, H.; Norouzi-Apourvari, S.; Salehi, F. Prediction of three-phase product yield of biomass pyrolysis using artificial intelligence-based models. *J. Anal. Appl. Pyrolysis* **2023**, *172*, 106015. [[CrossRef](#)]
13. Zhang, Y.; Ji, Y.; Qian, H. Progress in thermodynamic simulation and system optimization of pyrolysis and gasification of biomass. *Green Chem. Eng.* **2021**, *2*, 266–283. [[CrossRef](#)]
14. McCullough, K.; Williams, T.; Mingle, K.; Jamshidi, P.; Lauterbach, J. High-throughput experimentation meets artificial intelligence: A new pathway to catalyst discovery. *Phys. Chem. Chem. Phys.* **2020**, *22*, 11174–11196. [[CrossRef](#)]
15. Pan, I.; Pandey, D.S. Incorporating uncertainty in data driven regression models of fluidized bed gasification: A Bayesian approach. *Fuel Process. Technol.* **2016**, *142*, 305–314. [[CrossRef](#)]
16. Meena, M.; Shubham, S.; Paritosh, K.; Pareek, N.; Vivekanand, V. Production of biofuels from biomass: Predicting the energy employing artificial intelligence modelling. *Bioresour. Technol.* **2021**, *340*, 125642. [[CrossRef](#)]
17. Zhang, W.; Wu, Y.; Huang, S.; Wu, S.; Gao, J. Study on physicochemical characteristics, solidification and utilisation of tannery sludge gasification ash. *J. Environ. Manag.* **2022**, *310*, 114584. [[CrossRef](#)]
18. Courson, C.; Gallucci, K. Gas cleaning for waste applications (syngas cleaning for catalytic synthetic natural gas synthesis). In *Substitute Natural Gas from Waste*; Academic Press: Cambridge, MA, USA, 2019; pp. 161–220.
19. Brammer, J.G.; Bridgwater, A.V. Drying technologies for an integrated gasification bio-energy plant. *Renew. Sustain. Energy Rev.* **1999**, *3*, 243–289. [[CrossRef](#)]
20. Ascher, S.; Watson, I.; You, S. Machine learning methods for modelling the gasification and pyrolysis of biomass and waste. *Renew. Sustain. Energy Rev.* **2022**, *155*, 111902. [[CrossRef](#)]
21. Tang, F.; Chi, Y.; Jin, Y.; Zhu, Z.; Ma, J. Gasification characteristics of a simulated waste under separate and mixed atmospheres of steam and CO₂. *Fuel* **2022**, *317*, 123527. [[CrossRef](#)]
22. Glassman, I.; Yetter, R.A.; Glumac, N.G. *Combustion*; Academic Press: Cambridge, MA, USA, 2014.

23. Bukar, A.A.; Oumarou, M.B.; Tela, B.M.; Eljummah, A.M. Assessment of Biomass Gasification: A Review of Basic Design Considerations. *Am. J. Energy Res.* **2019**, *7*, 1–14.
24. Samiran, N.A.; Ng, J.-H.; Jaafar, M.N.M.; Valera-Medina, A.; Chong, C.T. H₂-rich syngas strategy to reduce NO_x and CO emissions and improve stability limits under premixed swirl combustion mode. *Int. J. Hydrogen Energy* **2016**, *41*, 19243–19255. [[CrossRef](#)]
25. Zhang, H.; Zhu, F.; Li, X.; Xu, R.; Li, L.; Yan, J.; Tu, X. Steam reforming of toluene and naphthalene as tar surrogate in a gliding arc discharge reactor. *J. Hazard. Mater.* **2019**, *369*, 244–253. [[CrossRef](#)] [[PubMed](#)]
26. Wongsiriamnuay, T.; Kannang, N.; Tippayawong, N. Effect of operating conditions on catalytic gasification of bamboo in a fluidized bed. *Int. J. Chem. Eng.* **2013**, *2013*, 297941. [[CrossRef](#)]
27. Ren, J.; Cao, J.-P.; Zhao, X.-Y.; Yang, F.-L.; Wei, X.-Y. Recent advances in syngas production from biomass catalytic gasification: A critical review on reactors, catalysts, catalytic mechanisms and mathematical models. *Renew. Sustain. Energy Rev.* **2019**, *116*, 109426. [[CrossRef](#)]
28. Silva, I.P.; Lima, R.M.; Silva, G.F.; Ruzene, D.S.; Silva, D.P. Thermodynamic equilibrium model based on stoichiometric method for biomass gasification: A review of model modifications. *Renew. Sustain. Energy Rev.* **2019**, *114*, 109305. [[CrossRef](#)]
29. Zhang, Y.; Li, B.; Li, H.; Liu, H. Thermodynamic evaluation of biomass gasification with air in autothermal gasifiers. *Thermochim. Acta* **2011**, *519*, 65–71. [[CrossRef](#)]
30. Lv, P.; Wang, J.; Bai, Y.; Song, X.; Su, W.; Yu, G.; Ma, Y. CO₂ gasification of petroleum coke with use of iron-based waste catalyst from FT synthesis. *Thermochim. Acta* **2022**, *711*, 179205. [[CrossRef](#)]
31. Zhang, Y.; Cui, Y.; Chen, P.; Liu, S.; Zhou, N.; Ding, K.; Fan, L.; Peng, P.; Min, M.; Cheng, Y.; et al. Gasification technologies and their energy potentials. In *Sustainable Resource Recovery and Zero Waste Approaches*; Elsevier: Amsterdam, The Netherlands, 2019; pp. 193–206.
32. Song, H.; Yang, G.; Xue, P.; Li, Y.; Zou, J.; Wang, S.; Yang, H.; Chen, H. Recent development of biomass gasification for H₂ rich gas production. *Appl. Energy Combust. Sci.* **2022**, *10*, 100059. [[CrossRef](#)]
33. Xu, G.; Yang, P.; Yang, S.; Wang, H.; Fang, B. Non-natural catalysts for catalytic tar conversion in biomass gasification technology. *Int. J. Hydrogen Energy* **2022**, *47*, 7638–7665. [[CrossRef](#)]
34. Budzianowski, W.M. Negative carbon intensity of renewable energy technologies involving biomass or carbon dioxide as inputs. *Renew. Sustain. Energy Rev.* **2012**, *16*, 6507–6521. [[CrossRef](#)]
35. Arnold, R.A.; Hill, J.M. Catalysts for gasification: A review. *Sustain. Energy Fuels* **2019**, *3*, 656–672. [[CrossRef](#)]
36. Galadima, A.; Masudi, A.; Muraza, O. Catalyst development for tar reduction in biomass gasification: Recent progress and the way forward. *J. Environ. Manag.* **2022**, *305*, 114274. [[CrossRef](#)]
37. Bao, X.; Shen, Z.; Zhang, H.; Liang, Q.; Liu, H. Evaluation of the catalytic effect and migration behavior of potassium in the molten slag during the char/molten slag interfacial gasification. *Fuel* **2022**, *307*, 121881. [[CrossRef](#)]
38. Wang, Y.-W.; Wang, Z.-Q.; Huang, J.-J.; Fang, Y.-T. Improved catalyst recovery combined with extracting alumina from Na₂CO₃-catalyzed gasification ash of a high-aluminium coal char. *Fuel* **2018**, *234*, 101–109. [[CrossRef](#)]
39. Mei, Y.; Zhang, Q.; Wang, Z.; Gao, S.; Fang, Y. Dancing and recrystallizing of Na₂CO₃ particles during catalytic gasification: Instructing the industrial catalysts loading procedures. *Fuel* **2022**, *316*, 123383.
40. Shen, S.U.; Wen, L.I.; Bai, Z.Q.; Xiang, H.W.; Jin, B.A.I. Production of hydrogen by steam gasification from lignin with Al₂O₃·Na₂O·xH₂O/NaOH/Al(OH)₃ catalyst. *J. Fuel Chem. Technol.* **2010**, *38*, 270–274.
41. Li, R.; Chen, Q.; Zhang, H. Detailed investigation on sodium (Na) species release and transformation mechanism during pyrolysis and char gasification of high-Na Zhundong coal. *Energy Fuels* **2017**, *31*, 5902–5912. [[CrossRef](#)]
42. Li, B.; Mbeugang, C.F.M.; Huang, Y.; Liu, D.; Wang, Q.; Zhang, S. A review of CaO based catalysts for tar removal during biomass gasification. *Energy* **2022**, *244*, 123172. [[CrossRef](#)]
43. Valizadeh, S.; Hakimian, H.; Cho, E.H.; Ko, C.H.; Lee, S.H.; Rhee, G.H.; Jung, S.-C.; Yoo, K.-S.; Park, Y.-K. Production of H₂-and CO-rich syngas from the CO₂ gasification of cow manure over (Sr/Mg)-promoted-Ni/Al₂O₃ catalysts. *Int. J. Hydrogen Energy* **2022**, *47*, 37218–37226. [[CrossRef](#)]
44. Ruivo, L.; Pio, D.; Yaremchenko, A.; Tarelho, L.; Frade, J.; Kantarelis, E.; Engvall, K. Iron-based catalyst (Fe₂-xNi_xTiO₅) for tar decomposition in biomass gasification. *Fuel* **2021**, *300*, 120859. [[CrossRef](#)]
45. Kou, J.; Feng, H.; Wei, W.; Wang, G.; Sun, J.; Jin, H.; Guo, L. Study on the detailed reaction pathway and catalytic mechanism of a Ni/ZrO₂ catalyst for supercritical water gasification of diesel oil. *Fuel* **2022**, *312*, 122849. [[CrossRef](#)]
46. Shan, Y.-Q.; Yin, L.-X.; Djandja, O.S.; Wang, Z.-C.; Duan, P.-G. Supercritical water gasification of waste water produced from hydrothermal liquefaction of microalgae over Ru catalyst for production of H₂ rich gas fuel. *Fuel* **2021**, *292*, 120288. [[CrossRef](#)]
47. Bocci, E.; Sisinni, M.; Moneti, M.; Vecchione, L.; Di Carlo, A.; Villarini, M. State of art of small scale biomass gasification power systems: A review of the different typologies. *Energy Procedia* **2014**, *45*, 247–256. [[CrossRef](#)]
48. Paredes-Sánchez, J.P.; López-Ochoa, L.M.; López-González, L.M.; Las-Heras-Casas, J.; Xiberta-Bernat, J. Evolution and perspectives of the bioenergy applications in Spain. *J. Clean. Prod.* **2019**, *213*, 553–568. [[CrossRef](#)]
49. Ingle, N.A.; Lakade, S.S. Design and development of downdraft gasifier to generate producer gas. *Energy Procedia* **2016**, *90*, 423–431. [[CrossRef](#)]
50. Zhou, P.; Li, J.; Chen, Q.; Wang, L.; Yang, J.; Wu, A.; Jiang, N.; Liu, Y.; Chen, J.; Zou, W.; et al. A comprehensive review of genus *Sanguisorba*: Traditional uses, chemical constituents and medical applications. *Front. Pharmacol.* **2021**, *12*, 750165. [[CrossRef](#)]

51. Pereira, E.G.; da Silva, J.N.; de Oliveira, J.L.; Machado, C.S. Sustainable energy: A review of gasification technologies. *Renew. Sustain. Energy Rev.* **2012**, *16*, 4753–4762. [[CrossRef](#)]
52. Mutlu, A.Y.; Yucel, O. An artificial intelligence based approach to predicting syngas composition for downdraft biomass gasification. *Energy* **2018**, *165*, 895–901. [[CrossRef](#)]
53. Hasanzadeh, R.; Mojaver, P.; Azdast, T.; Khalilarya, S.; Chitsaz, A. Developing gasification process of polyethylene waste by utilization of response surface methodology as a machine learning technique and multi-objective optimizer approach. *Int. J. Hydrogen Energy* **2023**, *48*, 5873–5886. [[CrossRef](#)]
54. Ascher, S.; Wang, X.; Watson, I.; Sloan, W.; You, S. Interpretable machine learning to model biomass and waste gasification. *Bioresour. Technol.* **2022**, *364*, 128062. [[CrossRef](#)]
55. Vasseghian, Y.; Bahadori, A.; Khataee, A.; Dragoi, E.-N.; Moradi, M. Modeling the interfacial tension of water-based binary and ternary systems at high pressures using a neuro-evolutionary technique. *ACS Omega* **2019**, *5*, 781–790. [[CrossRef](#)] [[PubMed](#)]
56. Altafini, C.R.; Wander, P.R.; Barreto, R.M. Prediction of the working parameters of a wood waste gasifier through an equilibrium model. *Energy Convers. Manag.* **2003**, *44*, 2763–2777. [[CrossRef](#)]
57. Sun, C.; Ai, L.; Liu, T. The PSO-ANN modeling study of highly valuable material and energy production by gasification of solid waste: An artificial intelligence algorithm approach. *Biomass Convers. Biorefin.* **2022**. [[CrossRef](#)]
58. Hai, T.; Alsharif, S.; Dhahad, H.A.; Attia, E.-A.; Shamseldin, M.A.; Ahmed, A.N. The evolutionary artificial intelligence-based algorithm to find the minimum GHG emission via the integrated energy system using the MSW as fuel in a waste heat recovery plant. *Sustain. Energy Technol. Assess.* **2022**, *53*, 102531. [[CrossRef](#)]
59. Hai, T.; Ali, M.A.; Zhou, J.; Dhahad, H.A.; Goyal, V.; Almojil, S.F.; Almohana, A.I.; Alali, A.F.; Almoalimi, K.T.; Ahmed, A.N. Feasibility and environmental assessments of a biomass gasification-based cycle next to optimization of its performance using artificial intelligence machine learning methods. *Fuel* **2023**, *334*, 126494. [[CrossRef](#)]
60. Ren, S.; Wu, S.; Weng, Q. Physics-informed machine learning methods for biomass gasification modeling by considering monotonic relationships. *Bioresour. Technol.* **2023**, *369*, 128472. [[CrossRef](#)]
61. Kargbo, H.O.; Zhang, J.; Phan, A.N. Optimisation of two-stage biomass gasification for hydrogen production via artificial neural network. *Appl. Energy* **2021**, *302*, 117567. [[CrossRef](#)]
62. Ayodele, B.V.; Mustapa, S.I.; Kanthasamy, R.; Mohammad, N.; AlTurki, A.; Babu, T.S. Performance analysis of support vector machine, Gaussian Process Regression, sequential quadratic programming algorithms in modeling hydrogen-rich syngas production from catalyzed co-gasification of biomass wastes from oil palm. *Int. J. Hydrogen Energy* **2022**, *47*, 41432–41443. [[CrossRef](#)]
63. Hlihor, R.M.; Diaconu, M.; Leon, F.; Curteanu, S.; Tavares, T.; Gavrilescu, M. Experimental analysis and mathematical prediction of Cd (II) removal by biosorption using support vector machines and genetic algorithms. *New Biotechnol.* **2015**, *32*, 358–368. [[CrossRef](#)]
64. Gaye, B.; Zhang, D.; Wulamu, A. Improvement of support vector machine algorithm in big data background. *Math. Probl. Eng.* **2021**, *2021*, 5594899. [[CrossRef](#)]
65. Awad, M.; Khanna, R. *Efficient Learning Machines: Theories, Concepts, and Applications for Engineers and System Designers*; Springer Nature: London, UK, 2015.
66. Ghosh, A.; Maiti, R. Soil erosion susceptibility assessment using logistic regression, decision tree and random forest: Study on the Mayurakshi river basin of Eastern India. *Environ. Earth Sci.* **2021**, *80*, 328. [[CrossRef](#)]
67. Fang, Y.; Ma, L.; Yao, Z.; Li, W.; You, S. Process optimization of biomass gasification with a Monte Carlo approach and random forest algorithm. *Energy Convers. Manag.* **2022**, *264*, 115734. [[CrossRef](#)]
68. Bhagat, S.K.; Tiyasha, T.; Tung, T.M.; Mostafa, R.R.; Yaseen, Z.M. Manganese (Mn) removal prediction using extreme gradient model. *Ecotoxicol. Environ. Saf.* **2020**, *204*, 111059. [[CrossRef](#)] [[PubMed](#)]
69. Ke, G.; Meng, Q.; Finley, T.; Wang, T.; Chen, W.; Ma, W.; Ye, Q.; Liu, T.Y. Lightgbm: A highly efficient gradient boosting decision tree. In Proceedings of the Advances in Neural Information Processing Systems 30, Long Beach, CA, USA, 4–9 December 2017.
70. Dorogush, A.V.; Ershov, V.; Gulin, A. CatBoost: Gradient boosting with categorical features support. *arXiv* **2018**, arXiv:1810.11363.
71. Bentéjac, C.; Csörgő, A.; Martínez-Muñoz, G. A comparative analysis of gradient boosting algorithms. *Artif. Intell. Rev.* **2021**, *54*, 1937–1967. [[CrossRef](#)]
72. Jiang, X.; Hu, J.; Jia, M.; Zheng, Y. Parameter matching and instantaneous power allocation for the hybrid energy storage system of pure electric vehicles. *Energies* **2018**, *11*, 1933. [[CrossRef](#)]
73. Li, Y.; Jia, M.; Han, X.; Bai, X.-S. Towards a comprehensive optimization of engine efficiency and emissions by coupling artificial neural network (ANN) with genetic algorithm (GA). *Energy* **2021**, *225*, 120331. [[CrossRef](#)]
74. Deng, J.; Deng, Y.; Cheong, K.H. Combining conflicting evidence based on Pearson correlation coefficient and weighted graph. *Int. J. Intell. Syst.* **2021**, *36*, 7443–7460. [[CrossRef](#)]
75. Shahbeik, H.; Rafiee, S.; Shafizadeh, A.; Jeddi, D.; Jafary, T.; Lam, S.S.; Pan, J.; Tabatabaei, M.; Aghbashlo, M. Characterizing sludge pyrolysis by machine learning: Towards sustainable bioenergy production from wastes. *Renew. Energy* **2022**, *199*, 1078–1092. [[CrossRef](#)]
76. Yang, Y.; Shahbeik, H.; Shafizadeh, A.; Masoudnia, N.; Rafiee, S.; Zhang, Y.; Pan, J.; Tabatabaei, M.; Aghbashlo, M. Biomass microwave pyrolysis characterization by machine learning for sustainable rural biorefineries. *Renew. Energy* **2022**, *201*, 70–86. [[CrossRef](#)]

77. Leng, L.; Zhang, W.; Liu, T.; Zhan, H.; Li, J.; Yang, L.; Li, J.; Peng, H.; Li, H. Machine learning predicting wastewater properties of the aqueous phase derived from hydrothermal treatment of biomass. *Bioresour. Technol.* **2022**, *358*, 127348. [[CrossRef](#)] [[PubMed](#)]
78. Prasertpong, P.; Onsree, T.; Khuenkaeo, N.; Tippayawong, N.; Lauterbach, J. Exposing and understanding synergistic effects in co-pyrolysis of biomass and plastic waste via machine learning. *Bioresour. Technol.* **2023**, *369*, 128419. [[CrossRef](#)] [[PubMed](#)]
79. Casalicchio, G.; Molnar, C.; Bischl, B. Visualizing the feature importance for black box models. In Proceedings of the Machine Learning and Knowledge Discovery in Databases: European Conference, ECML PKDD 2018, Dublin, Ireland, 10–14 September 2018; Proceedings, Part I 18; Springer International Publishing: New York, NY, USA, 2019.
80. Kim, J.Y.; Shin, U.H.; Kim, K. Predicting biomass composition and operating conditions in fluidized bed biomass gasifiers: An automated machine learning approach combined with cooperative game theory. *Energy* **2023**, *280*, 128138. [[CrossRef](#)]
81. Umenweke, G.C.; Afolabi, I.C.; Epelle, E.I.; Okolie, J.A. Machine learning methods for modeling conventional and hydrothermal gasification of waste biomass: A review. *Bioresour. Technol. Rep.* **2022**, *17*, 100976. [[CrossRef](#)]
82. Yang, Q.; Zhang, J.; Zhou, J.; Zhao, L.; Zhang, D. A hybrid data-driven machine learning framework for predicting the performance of coal and biomass gasification processes. *Fuel* **2023**, *346*, 128338. [[CrossRef](#)]
83. Aghbashlo, M.; Peng, W.; Tabatabaei, M.; Kalogirou, S.A.; Soltanian, S.; Hosseinzadeh-Bandbafha, H.; Mahian, O.; Lam, S.S. Machine learning technology in biodiesel research: A review. *Prog. Energy Combust. Sci.* **2021**, *85*, 100904. [[CrossRef](#)]
84. Yang, Y.; Shahbeik, H.; Shafizadeh, A.; Rafiee, S.; Hafezi, A.; Du, X.; Pan, J.; Tabatabaei, M.; Aghbashlo, M. Predicting municipal solid waste gasification using machine learning: A step toward sustainable regional planning. *Energy* **2023**, *278*, 127881. [[CrossRef](#)]
85. Sezer, S.; Kartal, F.; Özveren, U. Prediction of chemical exergy of syngas from downdraft gasifier by means of machine learning. *Therm. Sci. Eng. Prog.* **2021**, *26*, 101031. [[CrossRef](#)]
86. Chew, J.W.; Cocco, R.A. Application of machine learning methods to understand and predict circulating fluidized bed riser flow characteristics. *Chem. Eng. Sci.* **2020**, *217*, 115503. [[CrossRef](#)]
87. Sezer, S.; Özveren, U. Investigation of syngas exergy value and hydrogen concentration in syngas from biomass gasification in a bubbling fluidized bed gasifier by using machine learning. *Int. J. Hydrogen Energy* **2021**, *46*, 20377–20396. [[CrossRef](#)]
88. Wen, H.-T.; Lu, J.-H.; Phuc, M.-X. Applying artificial intelligence to predict the composition of syngas using rice husks: A comparison of artificial neural networks and gradient boosting regression. *Energies* **2021**, *14*, 2932. [[CrossRef](#)]
89. Aguado, R.; Casteleiro-Roca, J.-L.; Vera, D.; Calvo-Rolle, J.L. A hybrid intelligent model to predict the hydrogen concentration in the producer gas from a downdraft gasifier. *Int. J. Hydrogen Energy* **2022**, *47*, 20755–20770. [[CrossRef](#)]
90. Dong, L.; Wang, R.; Liu, P.; Sarvazizi, S. Prediction of Pyrolysis Kinetics of Biomass: New Insights from Artificial Intelligence-Based Modeling. *Int. J. Chem. Eng.* **2022**, *2022*, 6491745. [[CrossRef](#)]
91. Al-Wesabi, F.N.; Malibari, A.A.; Hilal, A.M.; Nemri, N.; Kumar, A.; Gupta, D. Intelligent ensemble of voting based solid fuel classification model for energy harvesting from agricultural residues. *Sustain. Energy Technol. Assess.* **2022**, *52*, 102040. [[CrossRef](#)]
92. Karimi, M.; Aminzadehsarikhanbeglou, E.; Vaferi, B. Robust intelligent topology for estimation of heat capacity of biochar pyrolysis residues. *Measurement* **2021**, *183*, 109857. [[CrossRef](#)]
93. Sezer, S.; Kartal, F.; Özveren, U. Artificial intelligence approach in gasification integrated solid oxide fuel cell cycle. *Fuel* **2022**, *311*, 122591. [[CrossRef](#)]
94. Hai, T.; Ali, M.A.; Alizadeh, A.; Zhou, J.; Dhahad, H.A.; Singh, P.K.; Almojil, S.F.; Almohana, A.I.; Alali, A.F.; Shamseldin, M. Recurrent neural networks optimization of biomass-based solid oxide fuel cells combined with the hydrogen fuel electrolyzer and reverse osmosis water desalination. *Fuel* **2023**, *346*, 128268. [[CrossRef](#)]
95. Kartal, F.; Özveren, U. Investigation of an integrated circulating fluidized bed gasifier/steam turbine/proton exchange membrane (PEM) fuel cell system for torrefied biomass and modeling with artificial intelligence approach. *Energy Convers. Manag.* **2022**, *263*, 115718. [[CrossRef](#)]
96. Ayub, Y.; Ren, J.; Shi, T.; Shen, W.; He, C. Poultry litter valorization: Development and optimization of an electro-chemical and thermal tri-generation process using an extreme gradient boosting algorithm. *Energy* **2023**, *263*, 125839. [[CrossRef](#)]
97. Hai, T.; Ali, M.A.; Alizadeh, A.; Dhahad, H.A.; Almojil, S.F.; Almohana, A.I.; Alali, A.F.; Goyal, V.; Farhang, B. Second law evaluation and environmental analysis of biomass-fired power plant hybridized with geothermal energy. *Sustain. Energy Technol. Assess.* **2023**, *56*, 102988. [[CrossRef](#)]
98. Kardani, N.; Zhou, A.; Nazem, M.; Lin, X. Modelling of municipal solid waste gasification using an optimised ensemble soft computing model. *Fuel* **2021**, *289*, 119903. [[CrossRef](#)]
99. Krzywanski, J.; Czakiert, T.; Nowak, W.; Shimizu, T.; Zylka, A.; Idziak, K.; Sosnowski, M.; Grabowska, K. Gaseous emissions from advanced CLC and oxyfuel fluidized bed combustion of coal and biomass in a complex geometry facility: A comprehensive model. *Energy* **2022**, *251*, 123896. [[CrossRef](#)]
100. Hai, T.; Dhahad, H.A.; Attia, E.-A.; Ibrahim, B.F.; Mohamed, A.; Almojil, S.F.; Almohana, A.I.; Alali, A.F.; Farhang, B. Proposal 3E analysis and multi-objective optimization of a new biomass-based energy system based on the organic cycle and ejector for the generation of sustainable power, heat, and cold. *Sustain. Energy Technol. Assess.* **2022**, *53*, 102551. [[CrossRef](#)]
101. Felix, C.B.; Chen, W.-H.; Ubando, A.T.; Park, Y.-K.; Lin, K.-Y.A.; Pugazhendhi, A.; Nguyen, T.-B.; Dong, C.-D. A comprehensive review of thermogravimetric analysis in lignocellulosic and algal biomass gasification. *Chem. Eng. J.* **2022**, *445*, 136730. [[CrossRef](#)]
102. Rabeti, S.M.; Manesh, M.K.; Amidpour, M. Techno-economic and environmental assessment of a novel polygeneration system based on integration of biomass air-steam gasification and solar parabolic trough collector. *Sustain. Energy Technol. Assess.* **2023**, *56*, 103030.

103. Hai, T.; Alsharif, S.; Aziz, K.H.H.; Dhahad, H.A.; Singh, P.K. Deep learning optimization of a biomass and biofuel-driven energy system with energy storage option for electricity, cooling, and desalinated water. *Fuel* **2023**, *334*, 126024. [[CrossRef](#)]
104. Ozbas, E.E.; Aksu, D.; Ongen, A.; Aydin, M.A.; Ozcan, H.K. Hydrogen production via biomass gasification, and modeling by supervised machine learning algorithms. *Int. J. Hydrogen Energy* **2019**, *44*, 17260–17268. [[CrossRef](#)]
105. Tiwary, S.; Ghugare, S.B.; Chavan, P.D.; Saha, S.; Datta, S.; Sahu, G.; Tambe, S.S. Co-gasification of high ash coal–biomass blends in a fluidized bed Gasifier: Experimental study and computational intelligence-based modeling. *Waste Biomass Valoriz.* **2020**, *11*, 323–341. [[CrossRef](#)]
106. Rezk, H.; Nassef, A.M.; Inayat, A.; Sayed, E.T.; Shahbaz, M.; Olabi, A. Improving the environmental impact of palm kernel shell through maximizing its production of hydrogen and syngas using advanced artificial intelligence. *Sci. Total Environ.* **2019**, *658*, 1150–1160. [[CrossRef](#)]
107. Zhao, S.; Zhang, Y.; Xu, W.; Gu, H. Experimental and artificial intelligence study on catalytic reforming of tar over bio-char surface coupled with hydrogen production. *Fuel* **2023**, *348*, 128563. [[CrossRef](#)]
108. Krzywanski, J.; Czakiert, T.; Zylka, A.; Nowak, W.; Sosnowski, M.; Grabowska, K.; Gao, Y. Modelling of SO₂ and NO_x emissions from coal and biomass combustion in Air-Firing, Oxyfuel, iG-CLC, and CLOU conditions by fuzzy logic approach. *Energies* **2022**, *15*, 8095. [[CrossRef](#)]
109. Karimi, M.; Alibak, A.H.; Alizadeh, S.M.S.; Sharif, M.; Vaferi, B. Intelligent modeling for considering the effect of bio-source type and appearance shape on the biomass heat capacity. *Measurement* **2022**, *189*, 110529. [[CrossRef](#)]
110. Ayub, H.M.U.; Park, S.J.; Binns, M. Biomass to syngas: Modified non-stoichiometric thermodynamic models for the downdraft biomass gasification. *Energies* **2020**, *13*, 5668. [[CrossRef](#)]
111. Chen, Y.; Yang, C.; Ying, K.; Yang, F.; Che, L.; Chen, Z. Prediction on microwave-assisted elimination of biomass tar using back propagation neural network. *Biomass Convers. Biorefin.* **2022**. [[CrossRef](#)]
112. Chen, W.-H.; Aniza, R.; Arpia, A.A.; Lo, H.-J.; Hoang, A.T.; Goodarzi, V.; Gao, J. A comparative analysis of biomass torrefaction severity index prediction from machine learning. *Appl. Energy* **2022**, *324*, 119689. [[CrossRef](#)]
113. Hai, T.; Mansir, I.B.; Yakooop, A.K.; Mulki, H.; Anqi, A.E.; Deifalla, A.; Chen, Y. Integration of wind turbine with biomass-fueled SOFC to provide hydrogen-rich fuel: Economic and CO₂ emission reduction assessment. *Process Saf. Environ. Prot.* **2023**, *170*, 946–959. [[CrossRef](#)]
114. Chew, J.W.; LaMarche, W.C.Q.; Cocco, R.A. 100 years of scaling up fluidized bed and circulating fluidized bed reactors. *Powder Technol.* **2022**, *409*, 117813. [[CrossRef](#)]
115. Hai, T.; El-Shafay, A.; Alizadeh, A.; Almojil, S.F.; Almohana, A.I.; Alali, A.F. Employing a booster/ejector-assisted organic flash cycle to heat recovery of SOFC system; Exergy-and economic-based optimization. *Int. J. Hydrogen Energy* **2023**, *48*, 18433–18453. [[CrossRef](#)]
116. Schneider, J.; Kirkpatrick, S. *Stochastic Optimization*; Springer Science & Business Media: New York, NY, USA, 2007.
117. Ben-Tal, A.; Ghaoui, L.E.; Nemirovski, A. *Robust Optimization*; Princeton University Press: Princeton, NJ, USA, 2009; Volume 28.
118. Chen, Z.; Kuhn, D.; Wiesemann, W. Data-driven chance constrained programs over Wasserstein balls. *Oper. Res.* **2022**. [[CrossRef](#)]
119. Bertsimas, D.; Gupta, V.; Kallus, N. Data-driven robust optimization. *Math. Program.* **2018**, *167*, 235–292. [[CrossRef](#)]
120. Lefevre, R.; Mariani, M.; Zambotti, L. Large deviations for renewal processes. *Stoch. Process. Their Appl.* **2011**, *121*, 2243–2271. [[CrossRef](#)]
121. Sheather, S.J.; Jones, M.C. A reliable data-based bandwidth selection method for kernel density estimation. *J. R. Stat. Soc. Ser. B* **1991**, *53*, 683–690. [[CrossRef](#)]
122. Ben-Hur, A.; Horn, D.; Siegelmann, H.T.; Vapnik, V. Support vector clustering. *J. Mach. Learn. Res.* **2001**, *2*, 125–137. [[CrossRef](#)]
123. Asaad, S.M.; Inayat, A.; Rocha-Meneses, L.; Jamil, F.; Ghenai, C.; Shanableh, A. Prospective of Response Surface Methodology as an Optimization Tool for Biomass Gasification Process. *Energies* **2022**, *16*, 40. [[CrossRef](#)]
124. Cheng, F.; Luo, H.; Colosi, L.M. Slow pyrolysis as a platform for negative emissions technology: An integration of machine learning models, life cycle assessment, and economic analysis. *Energy Convers. Manag.* **2020**, *223*, 113258. [[CrossRef](#)]
125. Ge, P. Analysis on approaches and structures of automated machine learning frameworks. In Proceedings of the 2020 International Conference on Communications, Information System and Computer Engineering (CISCE), Kuala Lumpur, Malaysia, 3–5 July 2020; IEEE: New York, NY, USA, 2020.
126. Feurer, M.; Eggenberger, K.; Falkner, S.; Lindauer, M.; Hutter, F. Auto-sklearn 2.0: The next generation. *arXiv* **2020**, arXiv:2007.04074 24.
127. Olson, R.S.; Moore, J.H. TPOT: A tree-based pipeline optimization tool for automating machine learning. In *Workshop on Automatic Machine Learning*; PMLR: London, UK, 2016.
128. Kotthoff, L.; Thornton, C.; Hoos, H.H.; Hutter, F.; Leyton-Brown, K. Auto-WEKA: Automatic model selection and hyperparameter optimization in WEKA. In *Automated Machine Learning: Methods, Systems, Challenges*; Springer: Cham, Switzerland, 2019; pp. 81–95.
129. Erickson, N.; Mueller, J.; Shirkov, A.; Zhang, H.; Larroy, P.; Li, M.; Smola, A. Autogluon-tabular: Robust and accurate automl for structured data. *arXiv* **2020**, arXiv:2003.06505.

Disclaimer/Publisher’s Note: The statements, opinions and data contained in all publications are solely those of the individual author(s) and contributor(s) and not of MDPI and/or the editor(s). MDPI and/or the editor(s) disclaim responsibility for any injury to people or property resulting from any ideas, methods, instructions or products referred to in the content.